nature chemical biology

ARTICLES

Targeted polypharmacology: discovery of dual inhibitors of tyrosine and phosphoinositide kinases

Beth Apsel[1], Jimmy A Blair[2], Beatriz Gonzalez[3,6], Tamim M Nazif[4], Morri E Feldman[1], Brian Aizenstein[5], Randy Hoffman[5], Roger L Williams[3], Kevan M Shokat[2,4] & Zachary A Knight[4,6]

The clinical success of multitargeted kinase inhibitors has stimulated efforts to identify promiscuous drugs with optimal selectivity profiles. It remains unclear to what extent such drugs can be rationally designed, particularly for combinations of targets that are structurally divergent. Here we report the systematic discovery of molecules that potently inhibit both tyrosine kinases and phosphatidylinositol-3-OH kinases, two protein families that are among the most intensely pursued cancer drug targets. Through iterative chemical synthesis, X-ray crystallography and kinome-level biochemical profiling, we identified compounds that inhibit a spectrum of new target combinations in these two families. Crystal structures revealed that the dual selectivity of these molecules is controlled by a hydrophobic pocket conserved in both enzyme classes and accessible through a rotatable bond in the drug skeleton. We show that one compound, PP121, blocks the proliferation of tumor cells by direct inhibition of oncogenic tyrosine kinases and phosphatidylinositol-3-OH kinases. These molecules demonstrate the feasibility of accessing a chemical space that intersects two families of oncogenes.

Tyrosine kinases promote cell growth, survival and proliferation, and are the target of frequent oncogenic mutations in tumors[1,2]. Eight tyrosine kinase inhibitors have been approved for clinical use, and dozens more are in late-stage development. As a critical part of their signaling function, most tyrosine kinases activate the lipid kinases of the phosphatidylinositol-3-OH kinase (PI(3)K) family[3]. PI(3)K family members include p110α, which is the most frequently mutated kinase in human cancer[4,5], and mTOR, which is a central regulator of cell growth[3]. In addition, the lipid phosphatase PTEN is a commonly inactivated tumor suppressor[6]. These observations have stimulated interest in the therapeutic potential of PI(3)K inhibitors, and the first such molecules recently entered clinical trials[7,8]. Together, PI(3)Ks and tyrosine kinases define an interconnected set of oncogenes that are the focus of intense drug discovery efforts.

We sought to discover molecules that potently inhibit both tyrosine kinases and PI(3)Ks. This investigation was motivated by two lines of reasoning. First, reactivation of PI(3)K signaling is a common mechanism of resistance to tyrosine kinase inhibitors[9–12], and pre-clinical studies have shown efficacy by combining inhibitors of these two families[13–16]. For this reason, molecules that target both tyrosine kinases and PI(3)Ks are likely to have potent antitumor activity.

Second, we sought to identify chemical principles that might guide the discovery of molecules targeting these two families of oncogenes. Though there are many examples of multitargeted kinase inhibitors, the targets of these drugs are not randomly distributed throughout the kinome[2,17–19]. Drugs that target certain combinations of kinases, but not others, tend to be repeatedly discovered. It would be desirable to instead rationally design promiscuous drugs based on the biological function of the targets, but it is unclear to what extent this can be achieved for proteins that are structurally divergent[20].

Protein kinases and PI(3)Ks diverged early in evolution[21] and therefore lack significant sequence similarity (**Fig. 1**). Nonetheless, these two enzyme families share several short motifs (for example, the DFG sequence that coordinates Mg^{2+}-ATP), and their kinase domains display a similar two-lobed architecture[22]. These enzymes also use a set of analogous residues to catalyze the phosphotransfer reaction, even though the orientation of key structural elements and the identity of most residues have diverged substantially (**Fig. 1**).

Consistent with these structural differences, there is limited overlap among known inhibitors of protein kinases and PI(3)Ks. A recent comprehensive profiling of kinase inhibitor selectivity tested 37 potent and structurally diverse protein kinase inhibitors against p110α and found that none were active[19]; in the same study, the p110α inhibitor PI-103 (**1**) showed little or no activity against over 300 protein kinases[19]. We have found that clinically approved protein kinase inhibitors bind to their primary target >10,000-fold more potently than any PI(3)K (**Supplementary Table 1** online). Nonetheless, pan-specific protein kinase inhibitors such as staurosporine (**2**) and

[1]Program in Chemistry and Chemical Biology, University of California, San Francisco, 600 16th Street, San Francisco, California 94158, USA. [2]Department of Chemistry, University of California, Berkeley, Berkeley, California 94720, USA. [3]MRC Laboratory of Molecular Biology, Hills Road, Cambridge CB2 2QH, UK. [4]Howard Hughes Medical Institute and Department of Cellular and Molecular Pharmacology, University of California, San Francisco, 600 16th Street, San Francisco, California 94158, USA. [5]Invitrogen Corporation, 501 Charmany Drive, Madison, Wisconsin 53719, USA. [6]Present addresses: Instituto de Química-Física Rocasolano (CSIC), Serrano 119, 28006 Madrid, Spain (B.G.) and The Rockefeller University, 1230 York Avenue, New York, New York 10021, USA (Z.A.K.). Correspondence should be addressed to K.M.S. (shokat@cmp.ucsf.edu).

Received 7 August; accepted 12 September; published online 12 October 2008; doi:10.1038/nchembio.117

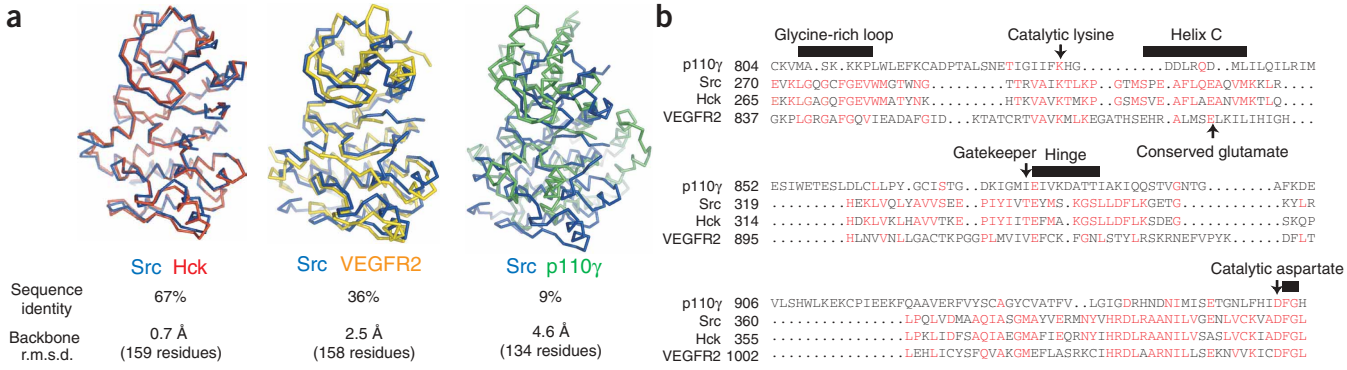

Figure 1 Structural and sequence comparison of tyrosine kinases and PI(3)Ks. (**a**) Backbone traces of crystal structures of the kinase domain of c-Src aligned to the kinase domain of the Src family tyrosine kinase Hck (left), the receptor tyrosine kinase VEGFR2 (center) and the PI(3)K p110γ (right). Statistics for the pairwise sequence identity and backbone r.m.s. deviation are shown below. The number of residues used for each alignment is shown in parentheses. (**b**) Sequence alignment of the kinase domains of the tyrosine kinases c-Src, Hck and VEGFR2 and the PI(3)K p110γ. Conserved residues relative to c-Src are colored red. The p110γ sequence was manually aligned to c-Src using X-ray structures of the two proteins that superimpose key secondary structural elements. The VEGFR2 insert comprising residues 940–997 is omitted.

quercetin (**3**) have been shown to inhibit PI(3)Ks at micromolar concentrations[23]. In addition, there are at least two reports of high-affinity interactions between a PI(3)K inhibitor and a protein kinase: wortmannin (**4**) inhibits the serine-threonine kinase PLK1 (ref. 24), and an imidazoquinoline (**5**) inhibits the serine-threonine kinase PDK1 (ref. 25). The structural basis for these interactions is not known.

We describe here the systematic discovery of small molecules that potently inhibit both tyrosine kinases and PI(3)Ks. We trace the unique selectivity of these molecules to interactions within a hydrophobic pocket that is conserved between both enzyme classes. We demonstrate that one such molecule, PP121 (**6**), blocks the proliferation of tumor cells through direct inhibition of oncogenic tyrosine kinases and PI(3)Ks, and further that this molecule evades a common mechanism of drug resistance by redundant inhibition of members of these two families.

RESULTS

Discovery of dual tyrosine kinase–PI(3)K inhibitors

We screened a library of tyrosine kinase inhibitors for activity against the PI(3)K p110α. This screen yielded two pyrazolopyrimidines, S1 (**7**) and S2 (**8**), that inhibit several PI(3)Ks at low micromolar concentrations (**Fig. 2a** and **Supplementary Table 1**). Structure-activity relationship (SAR) data revealed key elements of these hits required for PI(3)K inhibition. For example, substitution of the exocyclic amine (N4) with *N*-methyl abolished activity against PI(3)Ks, which suggests that this amino group may act as a hydrogen bond donor (**Fig. 2a**). At the R2 position, methyl and isopropyl but not *t*-butyl substituents were tolerated, placing steric constraint on substitution in that region.

The pyrazolopyrimidine is a well-characterized nucleus for tyrosine kinase inhibition[26–28], and we profiled S1 and S2 against over 200 protein kinases (**Fig. 2b**). These molecules displayed a selectivity pattern similar to that of the classical pyrazolopyrimidine kinase inhibitor PP1 (**9**; **Fig. 2b**), which inhibits Src family kinases, Abl and several receptor tyrosine kinases (for example, PDGFR and Ret) but is highly selective against the serine-threonine kinome.

Based on these data, we sought to optimize the potency and selectivity of S1 and S2. More than 200 analogs of these hits were iteratively synthesized through diversification of the R1 and R2 substituents (**Supplementary Table 1**). The progress of this chemistry was guided by testing each new compound against a panel of 14 tyrosine kinases and PI(3)Ks, monitoring this extensive SAR in order to identify chemical features that favor binding to both target classes, and then incorporating these features into subsequent rounds of analogs (**Supplementary Fig. 1** online).

From this effort we identified molecules that have novel target profiles against kinases in both families (**Fig. 2a**). This included dual inhibitors such as PP121 and PP487 (**10**) that inhibit, at nanomolar concentrations, both PI(3)Ks (for example, p110α and mTOR) and tyrosine kinases (for example, Src, Abl and the vascular endothelial growth factor (VEGF) receptor). We profiled PP121 and PP487 against over 200 protein kinases and found that they inhibit a pattern of tyrosine kinases similar to that inhibited by clinically approved drugs such as dasatinib (**11**) and sunitinib (**12**), yet they retain a high degree of selectivity against the serine-threonine kinome (**Fig. 2b**). Thus, these molecules are able to potently inhibit both tyrosine kinases and PI(3)Ks without indiscriminately targeting all kinases.

A selective mTOR inhibitor and other new target profiles

Although our goal was to identify molecules that inhibit both tyrosine kinases and PI(3)Ks, we discovered compounds with diverse and unexpected selectivity profiles (**Fig. 2a**). One such molecule is PP242 (**13**), which potently inhibited mTOR (half-maximal inhibitory concentration (IC_{50}) = 8 nM) but was much less active against other PI(3)K family members (**Fig. 2a**). Testing of this compound against 219 protein kinases revealed substantial selectivity relative to the protein kinome: at a concentration 100-fold above its IC_{50} for mTOR, PP242 inhibited only one kinase by more than 90% (Ret) and only three by more than 75% (PKCα, PKCβII and JAK2 V617F; **Fig. 2b** and **Supplementary Table 2** online). mTOR has emerged as an important drug target, and PP242 is the first selective and ATP-competitive inhibitor of mTOR that has been described. Unlike rapamycin, PP242 targets both mTOR complexes and therefore can be used to explore signaling by mTORC2. We treated BT549 cells with PP242 and found that this molecule inhibits the phosphorylation of Akt, the mTOR substrate p70S6K, and its downstream target S6 (**Supplementary Fig. 2** online). These data are consistent with a requirement for mTOR kinase activity in Akt phosphorylation[29], and we have used PP242 to dissect mTOR signaling (data not shown).

We were surprised by the diversity of target profiles that could be achieved by structural variation within the pyrazolopyrimidine chemotype (**Fig. 2a**). In many cases, small changes in structure produced considerable alterations in selectivity. For example, the DNA-PK–selective inhibitor PP162 (14) and the multitargeted dual inhibitor PP121 differ only in the arrangement of nitrogen atoms in the R1 ring (**Fig. 2a**). Conversely, the highly selective p110δ inhibitor PIK-294 (15) contains the pyrazolopyrimidine core embedded within a structure derived from an unrelated chemical series[18] (**Fig. 2a**). When PIK-294 is compared to tyrosine kinase–selective pyrazolopyrimidines such as PP20 (16), these two molecules span more than 10^8 fold in relative target selectivity (**Fig. 2a**).

To obtain a global view of the target selectivity of these molecules, we compared 172 pyrazolopyrimidines based on their IC_{50} values against 13 tyrosine kinases and PI(3)Ks using principal component analysis (PCA) (**Fig. 2c**). The proximity of compounds in this two-dimensional space provides a visual representation of their similarity against the 13 kinase targets, and we included as reference compounds four clinically approved tyrosine kinase inhibitors (sorafenib (17), gefitinib (18), dasatinib and sunitinib) and four widely used PI(3)K inhibitors (wortmannin, PI-103, IC87114 (19) and PIK-90 (20)). This analysis revealed that most pyrazolopyrimidines occupy a region of selectivity space intermediate between selective PI(3)K and tyrosine kinase inhibitors (**Fig. 2c**), which is consistent with the targeted profile of these compounds. By contrast, pyrazolopyrimidines such as PP20 and PIK294 that preferentially inhibit either PI(3)Ks or tyrosine kinases colocalized with reference compounds that are selective for either family (**Fig. 2c**). This provides an unbiased representation of the target profiles of these various classes of inhibitors.

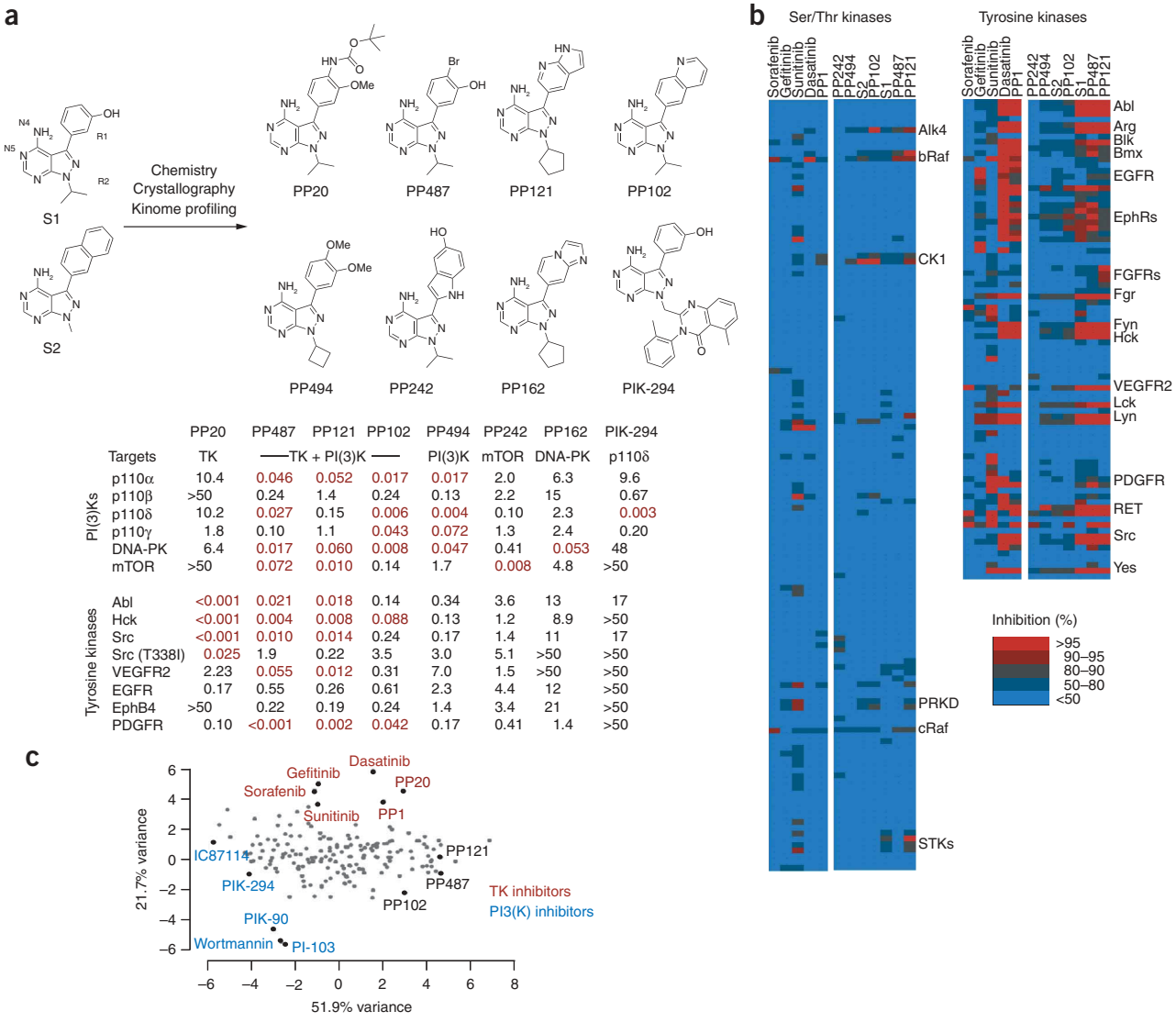

		PP20	PP487	PP121	PP102	PP494	PP242	PP162	PIK-294
	Targets	TK	TK + PI(3)K			PI(3)K	mTOR	DNA-PK	p110δ
PI(3)Ks	p110α	10.4	0.046	0.052	0.017	0.017	2.0	6.3	9.6
	p110β	>50	0.24	1.4	0.24	0.13	2.2	15	0.67
	p110δ	10.2	0.027	0.15	0.006	0.004	0.10	2.3	0.003
	p110γ	1.8	0.10	1.1	0.043	0.072	1.3	2.4	0.20
	DNA-PK	6.4	0.017	0.060	0.008	0.047	0.41	0.053	48
	mTOR	>50	0.072	0.010	0.14	1.7	0.008	4.8	>50
Tyrosine kinases	Abl	<0.001	0.021	0.018	0.14	0.34	3.6	13	17
	Hck	<0.001	0.004	0.008	0.088	0.13	1.2	8.9	>50
	Src	<0.001	0.010	0.014	0.24	0.17	1.4	11	17
	Src (T338I)	0.025	1.9	0.22	3.5	3.0	5.1	>50	>50
	VEGFR2	2.23	0.055	0.012	0.31	7.0	1.5	>50	>50
	EGFR	0.17	0.55	0.26	0.61	2.3	4.4	12	>50
	EphB4	>50	0.22	0.19	0.24	1.4	3.4	21	>50
	PDGFR	0.10	<0.001	0.002	0.042	0.17	0.41	1.4	>50

Figure 2 Biochemical target selectivity of pyrazolopyrimidine inhibitors. (**a**) Experimental strategy for the discovery of dual inhibitors, and IC_{50} values (μM) for 8 molecules tested against 14 tyrosine kinases and PI(3)Ks (10 μM ATP). IC_{50} values less than 0.1 μM are shaded red. Pyrazolopyrimidine N4 and N5, which make hydrogen bonds to the kinase, are labeled. (**b**) Percentage inhibition of 84 tyrosine kinases (right) and 135 serine-threonine kinases (left) by 7 inhibitors from this study (right columns) and 5 reference compounds (left columns). PP inhibitors were tested at 1 μM drug and, typically, 10 μM ATP. Data from the Invitrogen SelectScreen assay. (**c**) Principal component analysis of the target selectivity of 172 pyrazolopyrimidine inhibitors and 8 reference compounds. Key compounds are labeled.

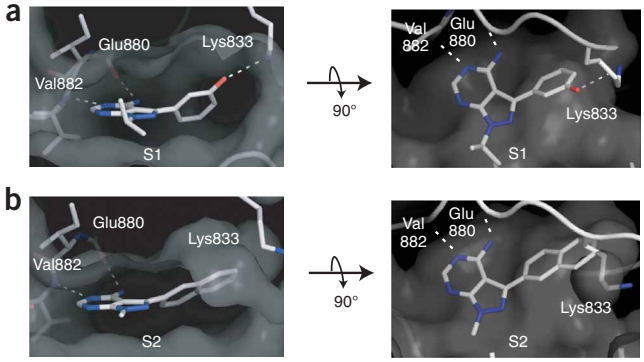

Figure 3 Crystal structures of S1 and S2 bound to human p110γ. (**a**) Binding mode of S1 to p110γ, viewed from the entrance to the ATP binding pocket (left) and above the ATP binding pocket (right). Dashed lines indicate hydrogen bonds. (**b**) Binding mode of S2 to p110γ.

Structure of pyrazolopyrimidines bound to p110γ

We determined crystal structures of S1 and S2 bound to p110γ in order to understand how this chemotype binds to PI(3)Ks (**Fig. 3** and **Supplementary Table 3** online). In these structures, the pyrazolopyrimidine N4 and N5 nitrogens make hydrogen bonds to the kinase hinge residues Glu880 and Val882, respectively (**Fig. 3**). Similar hydrogen bonds are made by adenine in ATP-bound structures[22], and these interactions account for SAR suggesting that the exocyclic amine at N4 is a hydrogen bond donor to PI(3)Ks.

The R1 aryl substituents of S1 and S2 project into a deeper pocket in p110γ that extends beyond the region occupied by ATP. In this region, the *m*-phenol of S1 makes a hydrogen bond to the catalytic lysine (Lys833 in p110γ), whereas the 2-naphthyl of S2 makes extensive hydrophobic interactions (**Fig. 3**). We have previously shown that chemically diverse PI(3)K inhibitors make interactions in this pocket that are required for high-affinity binding[18].

A gatekeeper for protein kinases but not PI(3)Ks

We sought to understand how molecules such as PP121 can potently inhibit both tyrosine kinases and PI(3)Ks but not serine-threonine kinases. Tyrosine and serine-threonine kinases are closely related to each other but only distantly related to the PI(3)K family[21]. For this reason, it was surprising that we were able to broaden the selectivity of pyrazolopyrimidines to target PI(3)Ks without introducing activity against the more numerous serine-threonine kinases. To account for this, we searched for structural features that are conserved between PI(3)Ks and tyrosine kinases and therefore may be used by these molecules to achieve their selectivity.

Within the protein kinase family, the selectivity of pyrazolopyrimidines is controlled by the size of a single amino acid, termed the gatekeeper[27,28]. Most tyrosine kinases have a small residue (threonine or valine) at this position and are more sensitive to these drugs, whereas most serine-threonine kinases have a larger residue (such as isoleucine or methionine) and are less sensitive. We tested the compounds in our panel against a T338I gatekeeper mutant of the tyrosine kinase Src and found that this mutation is sufficient to confer broad inhibitor resistance (**Fig. 4a**). Thus, the size of the gatekeeper residue controls the protein kinase selectivity of these drugs by preventing binding to most serine-threonine kinases.

PI(3)Ks have an isoleucine at the position that is structurally analogous to the gatekeeper within the PI(3)K family (**Fig. 1b**). For this reason, the potent inhibition of PI(3)Ks by the pyrazolopyrimidine chemotype was unexpected. We determined crystal structures of four compounds bound to c-Src (S1, PP121, PP102 (**21**) and PP494 (**22**)) and compared these with the structures of S1 and S2 bound to p110γ. Because c-Src and p110γ differ in many aspects of their structure (**Fig. 1a**), we focused first on analyzing only the relative orientation of the gatekeeper residue, the adenine of ATP and the drug within the active site of each kinase.

In the Src structures, the pyrazolopyrimidine superimposes with the adenine of ATP, positioning the R1 aryl substituent of the drug to project past the gatekeeper (Thr338) into the hydrophobic pocket (**Fig. 4b,c**). This is consistent with previously reported structures of pyrazolopyrimidines bound to tyrosine kinases[28]. When we compared this with the PI(3)K structures, we noticed that the residue analogous to the gatekeeper in PI(3)Ks (Ile879) is shifted both vertically and horizontally relative to its counterpart in protein kinases (**Fig. 4c**). This structural difference is accompanied by an alteration of the drug binding mode: the pyrazolopyrimidine core is displaced from alignment with ATP, and the R1 aryl substituent is rotated 90° (**Fig. 4b**). The combined effect of these structural differences and compound movements is that, in the PI(3)K structures, the R1 substituent of the drug projects underneath rather than adjacent to the side chain of the gatekeeper (**Fig. 4c**). This enables these molecules to make

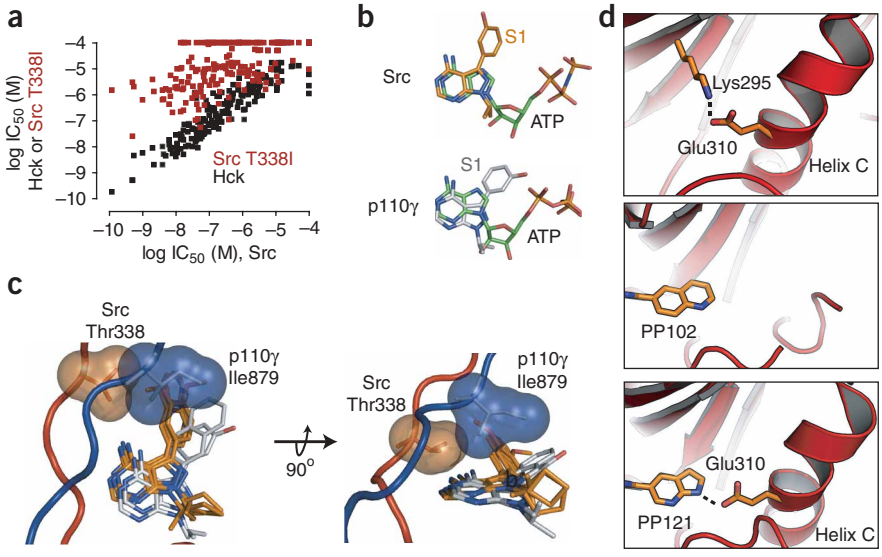

Figure 4 Structural comparison of pyrazolopyrimidine binding to tyrosine kinases and PI(3)Ks. (**a**) Correlation between IC_{50} values for inhibitors against Src (*x* axis) and either Hck or the gatekeeper mutant Src T338I (*y* axis). (**b**) Binding orientation of S1 relative to ATP in c-Src (top) and p110γ (bottom). (**c**) Overlay of cocrystal structures of inhibitors bound to c-Src (protein colored red, drugs orange: S1, PP102, PP121 and PP494) and p110γ (protein blue, compounds gray: S1 and S2). The gatekeeper residues Thr338 (c-Src) and Ile879 (p110γ) are highlighted. (**d**) Top, the catalytic lysine (Lys295) makes a hydrogen bond to Glu310 in active c-Src. Center, helix C and Glu310 are disordered in c-Src structures containing PP102. Bottom, PP121 makes a hydrogen bond to Glu310 and orders helix C when bound to c-Src.

interactions with the deeper hydrophobic pocket in PI(3)Ks despite the presence of a sterically demanding isoleucine at the gatekeeper position. This provides a structural rationale for the inhibition of PI(3)Ks, but not serine-threonine kinases, by the pyrazolopyrimidine chemotype.

Potent dual inhibitors target conserved catalytic residues

We synthesized many pyrazolopyrimidines, but only a few, such as PP121 and PP487, potently inhibit both tyrosine kinases and PI(3)Ks. We analyzed the cocrystal structures of these and related compounds in order to identify interactions that may contribute to their unique dual potency.

All protein kinases contain a conserved glutamic acid (Glu310 in Src) that makes a hydrogen bond to the catalytic lysine (Lys295 in Src). This interaction organizes the active site for catalysis and stabilizes helix C in an active conformation (**Fig. 4d**). The importance of these residues is underscored by their functional conservation across diverse kinases that share no sequence homology with the protein kinase superfamily[21]. Structures of pyrazolopyrimidines bound to protein kinases reveal that these drugs disrupt the interaction between Glu310 and Lys295, resulting in helix C adopting a disordered or inactive conformation (**Fig. 4d**). However, in the crystal structure of PP121 bound to Src, this molecule makes a hydrogen bond to Glu310, effectively substituting for the structural role of the catalytic lysine (**Fig. 4d**). This interaction has a substantial effect on the structure of the kinase; it results in the ordering of helix C and stabilization of an active conformation (**Fig. 4d** and **Supplementary Movie** online). It is likely that this interaction contributes to the more potent inhibition of tyrosine kinases by PP121 relative to closely related molecules such as PP102, which cannot make the same hydrogen bond.

We have not obtained a crystal structure of PP121 bound to p110γ, but a structurally analogous hydrogen bond is possible in PI(3)Ks (**Supplementary Fig. 3** online). This suggests that PP121 achieves its dual potency by targeting a residue (Glu310 in Src) that has been structurally conserved between kinase families. Notably, the compound S1 makes a hydrogen bond to two residues that are also highly conserved in each kinase family: the catalytic lysine in PI(3)Ks and the gatekeeper threonine in tyrosine kinases.

Based on these data, we propose that molecules such as PP121 achieve their dual selectivity by combining two molecular recognition steps. First, the size of the gatekeeper acts as a filter to block binding of pyrazolopyrimidines to most serine-threonine kinases. This filter does not block binding to PI(3)Ks, because the gatekeeper is in a different orientation in this kinase family. Second, the most potent dual inhibitors make specific hydrogen bonds to a small subset of residues, such as Lys295 and Glu310 in Src, that are conserved between protein and lipid kinases and that neighbor the gatekeeper pocket.

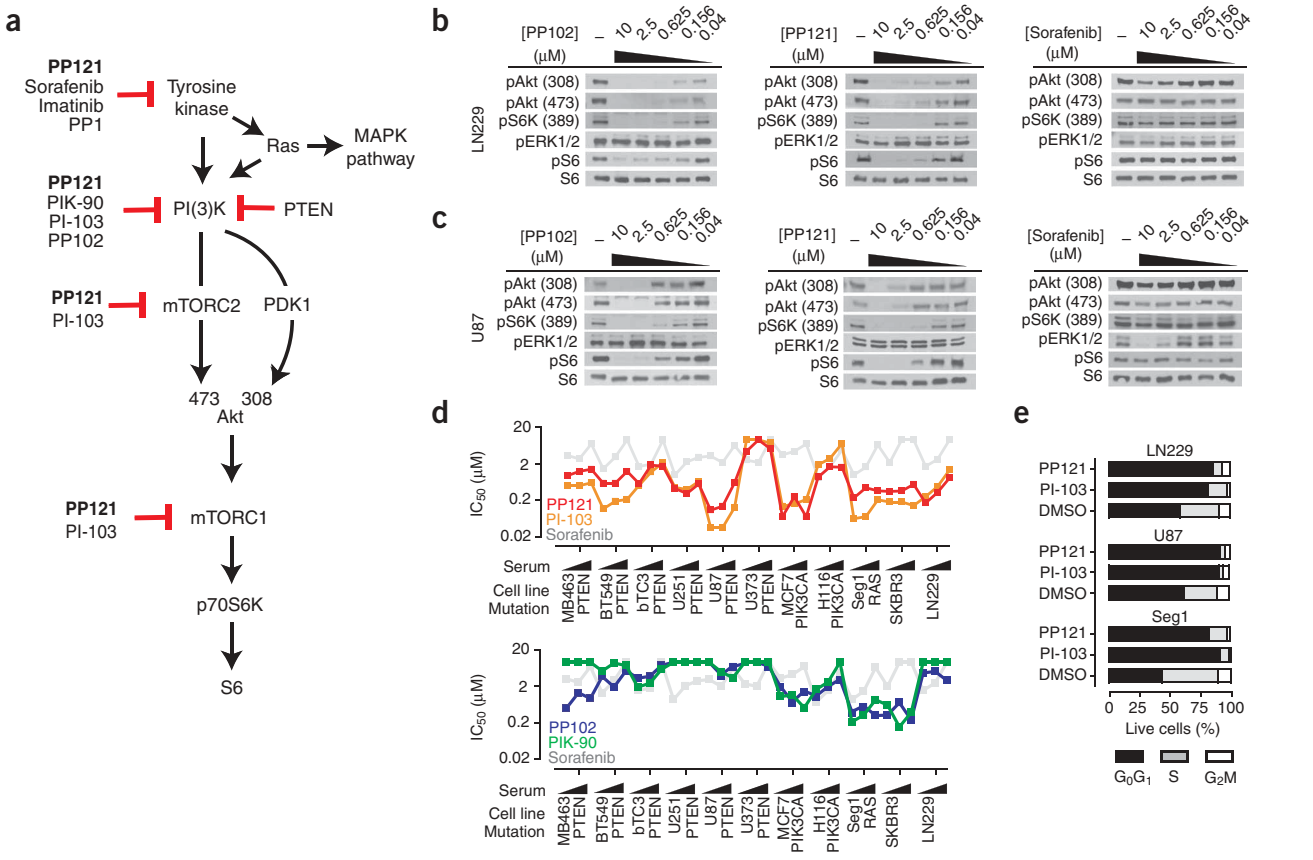

Figure 5 PP121 directly inhibits p110α/mTOR. (**a**) Schematic of signaling downstream of tyrosine kinases. Not all arrows represent direct physical interactions. Drugs used in this study and their key targets are highlighted. (**b**,**c**) LN229 (**b**) and U87 (**c**) glioblastoma cells in serum (10%) were treated with PP102 or PP121 (0.040 to 10 μM). Cells were lysed and phosphorylation of signaling proteins was probed by western blotting. pS6K (Ser235/236), pERK (Thr202/Tyr204). (**d**) Proliferation of tumor cells was measured following 72-h treatment with PP102, PP121, PI-103, PIK-90 or sorafenib (0.040 to 10 μM). Each cell line was tested at three serum concentrations (0.5%, 2% and 10%). (**e**) Cell cycle analysis by flow cytometry following treatment with PP121 or PI-103 (2.5 μM) or with vehicle (0.1% DMSO) for 24 h.

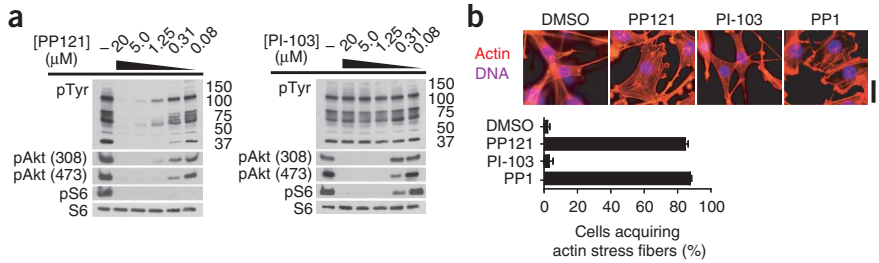

Figure 6 PP121 directly inhibits Src. (**a**) NIH3T3 cells transformed with v-Src(Thr338) were treated with the indicated concentration of each inhibitor (2 h), lysed and blotted for indicated proteins. Molecular weights are indicated adjacent to phosphotyrosine (pTyr) blots. (**b**) v-Src(Thr338)–transformed NIH3T3 cells were treated with the indicated inhibitors (2.5 μM, 24 h) and then stained for actin with fluorescein isothiocyanate (FITC)-phalloidin and for DNA with 4',6-diamidino-2-phenylindole (DAPI). The percentage of cells acquiring actin stress fibers was quantitated by counting while blinded to sample identity. Error bars are ± s.e.m. Scale bar is 20 μm.

PP121 inhibits PI(3)Ks and mTOR in tumor cells

We next explored the cellular effects of the dual inhibitor PP121. Our goal was to dissect the activity of this compound into distinct components resulting from direct inhibition of individual PI(3)Ks (for example, p110α and mTOR) or tyrosine kinases (for example, Src, Abl, Ret and the VEGF receptor). To do this, we systematically compared PP121 to six reference compounds (**Fig. 5a**). This panel includes three PI(3)K inhibitors (PIK-90, PI-103 and PP102) and three tyrosine kinase inhibitors (PP1, sorafenib and imatinib (**23**)) that each inhibit different subsets of kinases within these two families.

We first measured the effect of these drugs on signaling through the PI(3)K, mTOR and MAPK pathways in two glioblastoma cell lines, U87 and LN229 (**Fig. 4a–c**). PP121 and PP102 potently and dose-dependently blocked the phosphorylation of Akt, p70S6K and S6 in these cells (**Fig. 5b,c**). This inhibition was more potent in LN229 cells, which, unlike U87 cells, express functional PTEN (ref. 30) (**Fig. 5b,c**). We have observed a similar dose shift for the PI(3)K inhibitors PIK-90 and PI-103 in these two cell lines[31].

In contrast to their potent blockade of PI(3)K and mTOR signaling, PP121 and PP102 had no effect on the phosphorylation of Erk at concentrations up to 10 μM (**Fig. 5b,c**). This suggests that PP121 and PP102 block the PI(3)K pathway by direct inhibition of PI(3)K/mTOR in these cells, rather than through inhibition of an upstream tyrosine kinase. This conclusion is supported by the fact that the tyrosine kinase inhibitor sorafenib, which shares several targets with PP121 (for example, PDGFR, Ret and VEGFR2), had no effect on PI(3)K or mTOR signaling in these cells (**Fig. 5b,c**).

We next tested the ability of PP121 to block proliferation of a diverse panel of tumor cell lines containing mutations in the PI(3)K pathway components *PIK3CA*, *PTEN* or *KRAS*. Each cell line was assayed at three serum concentrations to explore the possibility that the requirement for PI(3)K signaling is magnified under conditions of growth factor deprivation[32].

PP121 potently inhibited the proliferation of a subset of these lines, and the pattern of its antiproliferative activity was similar to that of the dual PI(3)K-mTOR inhibitor PI-103 (**Fig. 5d**). The parallel activity of these two structurally unrelated molecules strongly suggests that they block cell proliferation through inhibition of a common target. By contrast, the tyrosine kinase inhibitor sorafenib was largely inactive (**Fig. 5d**).

We performed cell cycle analysis by flow cytometry to determine the nature of the proliferative block caused by these drugs. PP121 induced a G_0G_1 arrest in most tumor cells (**Fig. 5e**). This arrest was similar to the effect of treatment with PI-103 (**Fig. 5e**) and is characteristic of combined inhibition of PI(3)K and mTOR in these cells[31]. Together, these data demonstrate that PP121 blocks the proliferation of tumor cell lines containing PI(3)K pathway mutations by direct inhibition of PI(3)Ks and mTOR.

Direct inhibition of mTOR is likely to be particularly important for the antiproliferative activity of PP121. The PI(3)K inhibitors PP102 and PIK-90, which are less active against mTOR, also displayed less antiproliferative activity in these cells (**Fig. 5d**). In addition, we have shown previously that direct mTOR inhibition is required for robust blockade of cell proliferation by diverse PI(3)K family inhibitors[16,31]. Nonetheless, the molecular basis for this difference remains enigmatic, as PI(3)K inhibitors such as PP102 and PIK-90 potently block the phosphorylation of mTOR substrates (for example, Akt and p70S6K) indirectly via upstream PI(3)K inhibition[31] (**Fig. 5b,c**). In this respect, it is noteworthy that two of the first PI(3)K inhibitors to enter clinical trials, NVP-BEZ235 (**24**) and XL765, are also potent and direct mTOR inhibitors[8].

PP121 inhibits oncogenic Src and Ret

PP121 inhibits several tyrosine kinases that are prominent cancer drug targets, including Bcr-Abl, Src, Ret and the VEGF receptor (**Fig. 2a**). We therefore explored the activity of PP121 in cells that express these tyrosine kinases, in order to understand how this activity cooperates with inhibition of PI(3)Ks and mTOR.

Transformation of fibroblasts by the viral oncogene encoding v-Src results in dysregulated tyrosine phosphorylation and cytoskeletal rearrangements. As PP121 potently inhibits Src *in vitro* (IC_{50} = 14 nM; **Fig. 2a**), we tested the ability of PP121 to reverse v-Src–mediated cellular transformation. PP121 blocked tyrosine phosphorylation induced by v-Src and restored actin stress fiber staining, and the magnitude of these effects was similar to that observed after treatment with the Src family kinase inhibitor PP1 (**Fig. 6**). By contrast, PI-103 inhibited signaling through the PI(3)K/mTOR pathway but had no effect on either phosphotyrosine levels or cell morphology (**Fig. 6**). Thus, PP121 directly inhibits Src in cells and reverses its biochemical and morphological effects.

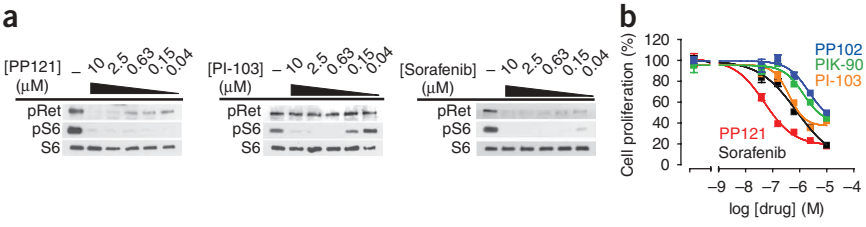

Figure 7 PP121 directly inhibits Ret. (**a**) TT thyroid carcinoma cells were treated with the indicated concentration of each inhibitor (2 h), lysed and blotted for indicated proteins. pRet (Tyr905). (**b**) TT cells were treated with a dose response of each inhibitor (0.040 to 10 μM), and cell number was quantitated after 13 d. Drug was replenished every 3 d. Error bars are ± s.e.m.

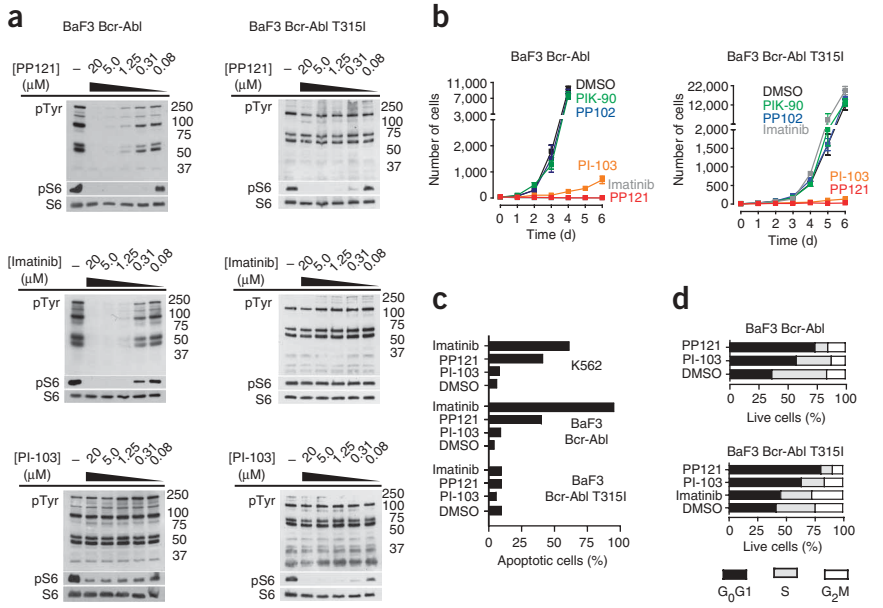

Figure 8 PP121 redundantly targets Bcr-Abl and PI(3)K/mTOR in CML cells. (**a**) BaF3 cells expressing Bcr-Abl (left column) or Bcr-Abl T315I (right column) were treated with PP121, PI-103 or imatinib (0.080 to 20 μM) for 120 min. Cells were lysed and phosphorylation of signaling proteins was probed by western blotting. (**b**) Proliferation of BaF3 Bcr-Abl and BaF3 Bcr-Abl T315I cells in response to selected drugs (2.5 μM). Error bars are ± s.e.m. (**c**) Percentage of cells undergoing apoptosis in response to drug treatment. BaF3 Bcr-Abl cells (2.5 μM, 36 h), BaF3 Bcr-Abl T315I and K562 cells (5 μM, 72 h). (**d**) Cell cycle analysis of live cells remaining after treatment in **c**.

Oncogenic mutations in the Ret receptor tyrosine kinase are frequently found in thyroid tumors[33], and PP121 potently inhibits the Ret kinase domain *in vitro* (IC_{50} < 1 nM). We therefore explored the activity of this compound in TT thyroid carcinoma cells that express the C634W oncogenic Ret mutant[34]. PP121 inhibited Ret autophosphorylation in cells at low nanomolar concentrations (**Fig. 7a**). This was similar to the effect of sorafenib (**Fig. 7a**), which is currently in clinical testing for thyroid cancer based in part on its activity against Ret kinase[33,35]. In contrast, the PI(3)K/mTOR inhibitor PI-103 blocked the phosphorylation of S6 but had no effect on Ret autophosphorylation (**Fig. 7a**).

We compared the ability of these compounds to block the proliferation of TT thyroid carcinoma cells (**Fig. 7b**). PP121 inhibited proliferation of these cells at low nanomolar concentrations (IC_{50} = 50 nM), whereas the Ret inhibitor sorafenib (IC_{50} = 780 nM) and the PI(3)K-mTOR inhibitor PI-103 (IC_{50} ~ 800 nM) were substantially less potent (**Fig. 7b**). The PI(3)K inhibitors PIK-90 (IC_{50} = 1.4 μM) and PP102 (IC_{50} = 2.2 μM) were active only at micromolar concentrations (**Fig. 7b**). The unique ability of PP121 to simultaneously inhibit Ret, PI(3)Ks and mTOR likely contributes to its exceptional potency in this setting.

PP121 directly inhibits the VEGF receptor

The VEGF receptor (VEGFR2) is a key target of two clinically approved small-molecule drugs (sunitinib and sorafenib), and PI(3)K/mTOR signaling is critical for VEGF-mediated angiogenesis[36,37]. As PP121 potently inhibits the VEGFR2 kinase domain *in vitro* (IC_{50} = 12 nM; **Fig. 2a**), we tested the ability of PP121 to block VEGF signaling in human umbilical vein endothelial cells (HUVECs) that endogenously express VEGFR2. PP121 potently blocked VEGF-stimulated activation of the PI(3)K and mitogen-activated protein kinase (MAPK) pathways (**Supplementary Fig. 4** online). In addition, PP121 inhibited VEGFR2 autophosphorylation at low nanomolar concentrations, thereby confirming that this molecule directly targets VEGFR2 in cells.

We compared the effects of PP121 with the closely related pyrazolopyrimidine PP102. This compound was less potent than PP121 against VEGFR2 *in vitro* but had similar activity against PI(3)Ks (**Fig. 2a**). Consistent with this selectivity profile, PP102 inhibited the phosphorylation of Akt and S6 in cells at low nanomolar concentrations but was much less potent at blocking the phosphorylation of VEGFR2 and Erk (**Supplementary Fig. 4**). We measured the effect of these compounds on the proliferation of endothelial cells stimulated with either complete medium or VEGF alone. PP121 and PP102 both inhibited HUVEC proliferation in complete medium at micromolar concentrations, but PP121 displayed a selective enhancement in potency against cells stimulated with only VEGF (IC_{50} = 41 nM; **Supplementary Fig. 4**). These data are consistent with more robust inhibition of VEGF signaling by PP121 relative to analogs such as PP102 that do not potently target VEGFR2.

Angiogenesis is a multistep process involving endothelial cell proliferation, migration and extracellular matrix (ECM) remodeling. We therefore tested these compounds in a functional angiogenesis assay that measures the ability of HUVECs to form three-dimensional tubes within a tumor-derived ECM. PP121 potently blocked tube formation in this assay (IC_{50} = 0.31 nM), whereas PI-103 and sorafenib were somewhat less active (IC_{50} = 0.60 and 0.59 nM, respectively). The selective PI(3)K inhibitors PIK-90 and PP102 inhibited tube formation only at micromolar concentrations (**Supplementary Fig. 4**). This spectrum of activities is consistent with multilevel collaboration between tyrosine kinases, PI(3)Ks and mTOR in angiogenic signaling.

PP121 overrides resistance in CML by redundant targeting

Chronic myelogenous leukemia (CML) is caused by a chromosomal translocation that generates the oncogene encoding Bcr-Abl[38]. Three clinically approved drugs target this tyrosine kinase, and each of these drugs is sensitive to an overlapping but distinct set of Bcr-Abl resistance mutations[39,40]. PP121 inhibits the Abl kinase *in vitro* (IC_{50} = 18 nM; **Fig. 2b**), and PI(3)K/mTOR signaling cooperates with Bcr-Abl to drive CML cell proliferation[15]. We therefore measured the activity of PP121 in cellular models of normal and drug-resistant CML in order to investigate the interplay between Bcr-Abl, PI(3)K and mTOR in this setting.

PP121 inhibited Bcr-Abl–induced tyrosine phosphorylation in K562 cells and BaF3 cells that express Bcr-Abl, and the potency of PP121 was similar to that of the clinically approved drug imatinib (**Fig. 8a** and **Supplementary Fig. 5** online). Consistent with this biochemical activity, PP121 robustly blocked the proliferation of both cell lines (**Fig. 8b** and **Supplementary Fig. 5**). This was the result of drug-induced apoptosis in K562 cells and a combination of apoptosis and cell cycle arrest in Bcr-Abl–expressing BaF3 cells (**Fig. 8c,d**).

In contrast to PP121, PI-103 did not block Bcr-Abl–mediated tyrosine phosphorylation but did inhibit signaling through the mTOR pathway (**Fig. 8a**). Correspondingly, PI-103 induced cell cycle arrest but not apoptosis (**Fig. 8c**,**d**). The PI(3)K inhibitors PIK-90 and PP102 had little effect on cell proliferation (**Fig. 8b**), which is consistent with their activity in other settings. Together, these data demonstrate that PP121, but not other PI(3)K or mTOR inhibitors, directly inhibits Bcr-Abl and thereby kills CML cells.

Clinical resistance to Bcr-Abl inhibitor therapy is caused by mutations in the kinase that prevent drug binding[39,40]. The most common resistance mutation is Bcr-Abl T315I, which increases the size of the gatekeeper residue from threonine to isoleucine. This mutation blocks the binding of all clinically approved kinase inhibitors and also confers resistance to inhibition by PP121 (IC_{50} > 1 μM; **Supplementary Table 2**). We tested PP121 in BaF3 cells that express Bcr-Abl T315I and found that this mutation abrogates the ability of PP121 to inhibit cellular tyrosine phosphorylation (**Fig. 8a**) and induce apoptosis (**Fig. 8c**). This confirms that the cytotoxicity of PP121 in CML cells is a consequence of direct Bcr-Abl inhibition; we obtained similar results with imatinib (**Fig. 8a**,**c**).

Unlike imatinib, however, PP121 retained the ability to potently block the proliferation of Bcr-Abl T315I–expressing cells (**Fig. 8b**). This proliferative block was due to a G_0G_1 cell cycle arrest that was similar to the effect of PI-103 treatment (**Fig. 8d**). Consistent with this arrest, PP121 potently inhibited the phosphorylation of S6 even in cells expressing Bcr-Abl T315I (**Fig. 8a**). We attribute this residual inhibition of S6 phosphorylation to direct inhibition of mTOR by PP121 that is unaffected by Bcr-Abl mutation. Thus, PP121 is able to evade drug resistance caused by mutation of a single kinase by redundantly targeting two pathways: Bcr-Abl–mediated cell survival and mTOR-mediated cell proliferation. This mechanism of action is complementary to ongoing efforts to identify inhibitors that target specific Bcr-Abl mutants[41].

DISCUSSION

Effective therapy for many cancers will require the simultaneous inhibition of multiple oncogenic kinases[9,10,31,41,42]. This is because tumor cells rapidly develop resistance to inhibitors of individual kinases, either through mutation of the target to prevent drug binding[39,40], activation of surrogate kinases to substitute for the drug target[9], or modulation of pathway components to buffer against incomplete inhibition[10]. Even in the absence of acquired resistance, there are few examples of selective kinase inhibitors that have substantial antitumor activity as monotherapy, which indicates that inhibition of additional targets will be required[1,42].

Multitargeted drugs will be an important tool in meeting this challenge[43–45], but it is unclear to what extent the selectivity of these molecules can be rationally designed, particularly for combinations of targets that are structurally divergent[2,20]. Progress toward this goal will require (i) the discovery of chemical and structural features that link important classes of drug targets, and (ii) the use of these features to guide the design of promiscuous drugs with customized selectivity profiles. The chemical principles that will enable this type of targeted polypharmacology remain largely unknown, but the successful pursuit of single-targeted kinase inhibitors provides reason for optimism. In that setting, the early identification of key selectivity determinants, such as the inactive conformation[43,44], allosteric sites[45], reactive cysteine residues[46,47] and the gatekeeper[27,28], has now led to the systematic design of molecules that target these features.

We investigated whether it would be possible to discover molecules that target both tyrosine kinases and PI(3)Ks. These two protein families are among the most intensely pursued cancer drug targets, but they are substantially more divergent than the typical targets of multitargeted drugs. We show here that it is possible to identify potent, selective and drug-like molecules that target these two families of oncogenic kinases, and we further elucidate the structural features that control the unique selectivity of these molecules. This expands the landscape of target selectivities that are accessible to rational drug design. As several clinically approved kinase inhibitors are believed to act through serendipitous target combinations, exploration of such chemical space may be a productive strategy for discovering molecules with emergent properties.

METHODS

Chemical synthesis. All compounds were synthesized from commercially available starting materials and purified by RP-HPLC. See **Supplementary Methods** online for complete details.

***In vitro* kinase assays.** For IC_{50} value determinations, purified kinase domains were incubated with inhibitors at two-fold or four-fold dilutions over a concentration range of 50 μM to 0.001 μM or with vehicle (0.1% DMSO) in the presence of 10 μM ATP, 2.5 μCi of [γ-^{32}P]ATP and substrate. Reactions were terminated by spotting onto nitrocellulose or phosphocellulose membranes, depending on the substrate; this membrane was then washed five or six times to remove unbound radioactivity and dried. Transferred radioactivity was quantitated by phosphorimaging, and IC_{50} values were calculated by fitting the data to a sigmoidal dose-response using Prism (GraphPad). Single concentration kinome profiling was performed using the Invitrogen SelectScreen assay.

X-ray crystallography. p110γ and Src were recombinantly expressed, purified and crystallized in the presence of inhibitors by hanging-drop vapor diffusion. Structures were solved from diffraction data by molecular replacement. See **Supplementary Methods** for additional details.

Cell culture and western blot analysis. Cells were grown in 12-well plates and treated with inhibitor at the indicated concentrations or with vehicle (0.1% DMSO). Treated cells were lysed, and lysates were resolved by SDS-PAGE, transferred to nitrocellulose and blotted. All antibodies were purchased from Cell Signaling Technology.

Cell proliferation assays. Cells grown in 96-well plates were treated with inhibitor at four-fold dilutions (10 μM to 0.040 μM) or vehicle (0.1% DMSO). After 72 h, cells were exposed to Resazurin sodium salt (22 μM, Sigma), and fluorescence was quantified. IC_{50} values were calculated using Prism. For proliferation assays involving single-cell counting, non-adherent cells were plated at low density (3–5% confluence) and treated with drug (2.5 μM) or vehicle (0.1% DMSO). Cells were diluted into trypan blue daily, and viable cells were counted using a hemocytometer.

Apoptosis and cell cycle analysis. Cells were treated with the indicated concentration of inhibitor or vehicle (0.1% DMSO) for 24 to 72 h. Cells were either stained live with AnnexinV-FITC or fixed with ethanol and stained with propidium iodide. Cell populations were separated using a FacsCalibur flow cytometer; data was collected using CellQuest Pro (BD Biosciences) and analyzed with either ModFit (Verity Software House) or FlowJo (Tree Star Inc.).

Accession codes. Protein Data Bank: Coordinates have been deposited under the following accession codes: p110γ bound to S1, 2V4L; p110γ bound to S2, 3ENE; c-Src bound to PP121, 3EN4; c-Src bound to PP494, 3EN5; c-Src bound to PP102, 3EN6; c-Src bound to S1, 3EN7.

Note: Supplementary information and chemical compound information is available on the Nature Chemical Biology website.

ACKNOWLEDGMENTS

We thank W.A. Weiss (University of California, San Francisco) for providing glioblastoma cells, W.M. Korn (University of California, San Francisco) for providing Seg1 cells, N. Shah (University of California, San Francisco) for

providing BaF3 Bcr-Abl and BaF3 Bcr-Abl T315I cells, and D. Hanahan (University of California, San Francisco) for βTC3 cells. We thank P.J. Alaimo (Seattle University) for synthetic intermediates that were used to prepare several compounds, and J.L. Garrison for helpful comments on the text. This work was supported by the Sandler Program in Asthma Research and US National Institutes of Health grant AI44009. Mass spectrometry was made possible by US National Institutes of Health shared resource grants NCRR RR015804 and NCRR RR001614. B.G. has a Ramon y Cajal fellowship from the Ministerio de Educación y Ciencia in Spain and received funding from Comunidad Autonoma de Madrid-CSIC (CCG07-CSIC/GEN-2232).

AUTHOR CONTRIBUTIONS

B. Apsel and Z.A.K. synthesized the molecules, determined their IC_{50} values and performed cell proliferation assays. Z.A.K. performed the western blots. B. Apsel performed flow cytometry, angiogenesis and imaging assays. B.G. and R.L.W. determined the PI(3)K cocrystal structures. B. Apsel and J.A.B. determined the Src cocrystal structures. T.M.N. performed the HUVEC blots. B. Aizenstein and R.H. performed the Invitrogen SelectScreen. M.E.F. assisted with data analysis. Z.A.K. designed the experiments and wrote the paper, with input from B. Apsel and K.M.S.

COMPETING INTERESTS STATEMENT

The authors declare competing financial interests: details accompany the full-text HTML version of the paper at http://www.nature.com/naturechemicalbiology/.

Published online at http://www.nature.com/naturechemicalbiology/
Reprints and permissions information is available online at http://npg.nature.com/reprintsandpermissions/

1. Krause, D.S. & Van Etten, R.A. Tyrosine kinases as targets for cancer therapy. *N. Engl. J. Med.* **353**, 172–187 (2005).
2. Sebolt-Leopold, J.S. & English, J.M. Mechanisms of drug inhibition of signalling molecules. *Nature* **441**, 457–462 (2006).
3. Shaw, R.J. & Cantley, L.C. Ras, PI(3)K and mTOR signalling controls tumour cell growth. *Nature* **441**, 424–430 (2006).
4. Samuels, Y. *et al.* High frequency of mutations of the PIK3CA gene in human cancers. *Science* **304**, 554 (2004).
5. Samuels, Y. & Velculescu, V.E. Oncogenic mutations of PIK3CA in human cancers. *Cell Cycle* **3**, 1221–1224 (2004).
6. Li, J. *et al.* PTEN, a putative protein tyrosine phosphatase gene mutated in human brain, breast, and prostate cancer. *Science* **275**, 1943–1947 (1997).
7. Knight, Z.A. & Shokat, K.M. Chemically targeting the PI3K family. *Biochem. Soc. Trans.* **35**, 245–249 (2007).
8. Maira, S.M. *et al.* Identification and characterization of NVP-BEZ235, a new orally available dual phosphatidylinositol 3-kinase/mammalian target of rapamycin inhibitor with potent *in vivo* antitumor activity. *Mol. Cancer Ther.* **7**, 1851–1863 (2008).
9. Engelman, J.A. *et al.* MET amplification leads to gefitinib resistance in lung cancer by activating ERBB3 signaling. *Science* **316**, 1039–1043 (2007).
10. Sergina, N.V. *et al.* Escape from HER-family tyrosine kinase inhibitor therapy by the kinase-inactive HER3. *Nature* **445**, 437–441 (2007).
11. Haas-Kogan, D.A. *et al.* Epidermal growth factor receptor, protein kinase B/Akt, and glioma response to erlotinib. *J. Natl. Cancer Inst.* **97**, 880–887 (2005).
12. Mellinghoff, I.K. *et al.* Molecular determinants of the response of glioblastomas to EGFR kinase inhibitors. *N. Engl. J. Med.* **353**, 2012–2024 (2005).
13. Fan, Q.W. *et al.* Combinatorial efficacy achieved through two-point blockade within a signaling pathway-a chemical genetic approach. *Cancer Res.* **63**, 8930–8938 (2003).
14. Wang, M.Y. *et al.* Mammalian target of rapamycin inhibition promotes response to epidermal growth factor receptor kinase inhibitors in PTEN-deficient and PTEN-intact glioblastoma cells. *Cancer Res.* **66**, 7864–7869 (2006).
15. Mohi, M.G. *et al.* Combination of rapamycin and protein tyrosine kinase (PTK) inhibitors for the treatment of leukemias caused by oncogenic PTKs. *Proc. Natl. Acad. Sci. USA* **101**, 3130–3135 (2004).
16. Fan, Q.W. *et al.* A dual phosphoinositide-3-kinase alpha/mTOR inhibitor cooperates with blockade of epidermal growth factor receptor in PTEN-mutant glioma. *Cancer Res.* **67**, 7960–7965 (2007).
17. Knight, Z.A. & Shokat, K.M. Features of selective kinase inhibitors. *Chem. Biol.* **12**, 621–637 (2005).
18. Knight, Z.A. *et al.* A pharmacological map of the PI3-K family defines a role for p110alpha in insulin signaling. *Cell* **125**, 733–747 (2006).
19. Karaman, M.W. *et al.* A quantitative analysis of kinase inhibitor selectivity. *Nat. Biotechnol.* **26**, 127–132 (2008).
20. Hopkins, A.L., Mason, J.S. & Overington, J.P. Can we rationally design promiscuous drugs? *Curr. Opin. Struct. Biol.* **16**, 127–136 (2006).
21. Scheeff, E.D. & Bourne, P.E. Structural evolution of the protein kinase-like superfamily. *PLoS Comput. Biol.* **1**, e49 (2005).
22. Walker, E.H., Perisic, O., Ried, C., Stephens, L. & Williams, R.L. Structural insights into phosphoinositide 3-kinase catalysis and signalling. *Nature* **402**, 313–320 (1999).
23. Walker, E.H. *et al.* Structural determinants of phosphoinositide 3-kinase inhibition by wortmannin, LY294002, quercetin, myricetin, and staurosporine. *Mol. Cell* **6**, 909–919 (2000).
24. Liu, Y. *et al.* Wortmannin, a widely used phosphoinositide 3-kinase inhibitor, also potently inhibits mammalian polo-like kinase. *Chem. Biol.* **12**, 99–107 (2005).
25. Stauffer, F., Maira, S.M., Furet, P. & Garcia-Echeverria, C. Imidazo[4,5-c]quinolines as inhibitors of the PI3K/PKB-pathway. *Bioorg. Med. Chem. Lett.* **18**, 1027–1030 (2008).
26. Hanke, J.H. *et al.* Discovery of a novel, potent, and Src family-selective tyrosine kinase inhibitor. Study of Lck- and FynT-dependent T cell activation. *J. Biol. Chem.* **271**, 695–701 (1996).
27. Liu, Y. *et al.* Structural basis for selective inhibition of Src family kinases by PP1. *Chem. Biol.* **6**, 671–678 (1999).
28. Schindler, T. *et al.* Crystal structure of Hck in complex with a Src family-selective tyrosine kinase inhibitor. *Mol. Cell* **3**, 639–648 (1999).
29. Sarbassov, D.D., Guertin, D.A., Ali, S.M. & Sabatini, D.M. Phosphorylation and regulation of Akt/PKB by the rictor-mTOR complex. *Science* **307**, 1098–1101 (2005).
30. Ishii, N. *et al.* Frequent co-alterations of TP53, p16/CDKN2A, p14ARF, PTEN tumor suppressor genes in human glioma cell lines. *Brain Pathol.* **9**, 469–479 (1999).
31. Fan, Q.W. *et al.* A dual PI3 kinase/mTOR inhibitor reveals emergent efficacy in glioma. *Cancer Cell* **9**, 341–349 (2006).
32. Samuels, Y. *et al.* Mutant PIK3CA promotes cell growth and invasion of human cancer cells. *Cancer Cell* **7**, 561–573 (2005).
33. Carlomagno, F. *et al.* BAY 43–9006 inhibition of oncogenic RET mutants. *J. Natl. Cancer Inst.* **98**, 326–334 (2006).
34. Carlomagno, F. *et al.* Point mutation of the RET proto-oncogene in the TT human medullary thyroid carcinoma cell line. *Biochem. Biophys. Res. Commun.* **207**, 1022–1028 (1995).
35. Gupta-Abramson, V. *et al.* Phase II trial of sorafenib in advanced thyroid cancer. *J. Clin. Oncol.* (in the press).
36. Graupera, M. *et al.* Angiogenesis selectively requires the p110alpha isoform of PI3K to control endothelial cell migration. *Nature* **453**, 662–666 (2008).
37. Guba, M. *et al.* Rapamycin inhibits primary and metastatic tumor growth by antiangiogenesis: involvement of vascular endothelial growth factor. *Nat. Med.* **8**, 128–135 (2002).
38. de Klein, A. *et al.* A cellular oncogene is translocated to the Philadelphia chromosome in chronic myelocytic leukaemia. *Nature* **300**, 765–767 (1982).
39. Shah, N.P. *et al.* Multiple BCR-ABL kinase domain mutations confer polyclonal resistance to the tyrosine kinase inhibitor imatinib (STI571) in chronic phase and blast crisis chronic myeloid leukemia. *Cancer Cell* **2**, 117–125 (2002).
40. Gorre, M.E. *et al.* Clinical resistance to STI-571 cancer therapy caused by BCR-ABL gene mutation or amplification. *Science* **293**, 876–880 (2001).
41. Sawyers, C.L. Cancer: mixing cocktails. *Nature* **449**, 993–996 (2007).
42. Stommel, J.M. *et al.* Coactivation of receptor tyrosine kinases affects the response of tumor cells to targeted therapies. *Science* **318**, 287–290 (2007).
43. Schindler, T. *et al.* Structural mechanism for STI-571 inhibition of abelson tyrosine kinase. *Science* **289**, 1938–1942 (2000).
44. Liu, Y. & Gray, N.S. Rational design of inhibitors that bind to inactive kinase conformations. *Nat. Chem. Biol.* **2**, 358–364 (2006).
45. Dudley, D.T., Pang, L., Decker, S.J., Bridges, A.J. & Saltiel, A.R. A synthetic inhibitor of the mitogen-activated protein kinase cascade. *Proc. Natl. Acad. Sci. USA* **92**, 7686–7689 (1995).
46. Fry, D.W. *et al.* Specific, irreversible inactivation of the epidermal growth factor receptor and erbB2, by a new class of tyrosine kinase inhibitor. *Proc. Natl. Acad. Sci. USA* **95**, 12022–12027 (1998).
47. Cohen, M.S., Zhang, C., Shokat, K.M. & Taunton, J. Structural bioinformatics-based design of selective, irreversible kinase inhibitors. *Science* **308**, 1318–1321 (2005).